FERMILAB-PUB-13-122-E

Measurement of the top-quark pair production cross-section in events with two leptons and bottom-quark jets using the full CDF data set

T. Aaltonen,[21] S. Amerio,[40] D. Amidei,[32] A. Anastassov[x],[15] A. Annovi,[17] J. Antos,[12] G. Apollinari,[15] J.A. Appel,[15] T. Arisawa,[53] A. Artikov,[13] J. Asaadi,[48] W. Ashmanskas,[15] B. Auerbach,[2] A. Aurisano,[48] F. Azfar,[39] W. Badgett,[15] T. Bae,[25] A. Barbaro-Galtieri,[26] V.E. Barnes,[44] B.A. Barnett,[23] P. Barria[hh],[42] P. Bartos,[12] M. Bauce[ff],[40] F. Bedeschi,[42] S. Behari,[15] G. Bellettini[gg],[42] J. Bellinger,[55] D. Benjamin,[14] A. Beretvas,[15] A. Bhatti,[46] K.R. Bland,[5] B. Blumenfeld,[23] A. Bocci,[14] A. Bodek,[45] D. Bortoletto,[44] J. Boudreau,[43] A. Boveia,[11] L. Brigliadori[ee],[6] C. Bromberg,[33] E. Brucken,[21] J. Budagov,[13] H.S. Budd,[45] K. Burkett,[15] G. Busetto[ff],[40] P. Bussey,[19] P. Butti[gg],[42] A. Buzatu,[19] A. Calamba,[10] S. Camarda,[4] M. Campanelli,[28] F. Canelli[oo],[11,15] B. Carls,[22] D. Carlsmith,[55] R. Carosi,[42] S. Carrillo[m],[16] B. Casal[k],[9] M. Casarsa,[49] A. Castro[ee],[6] P. Catastini,[20] D. Cauz,[49] V. Cavaliere,[22] M. Cavalli-Sforza,[4] A. Cerri[f],[26] L. Cerrito[s],[28] Y.C. Chen,[1] M. Chertok,[7] G. Chiarelli,[42] G. Chlachidze,[15] K. Cho,[25] D. Chokheli,[13] M.A. Ciocci[hh],[42] A. Clark,[18] C. Clarke,[54] M.E. Convery,[15] J. Conway,[7] M. Corbo,[15] M. Cordelli,[17] C.A. Cox,[7] D.J. Cox,[7] M. Cremonesi,[42] D. Cruz,[48] J. Cuevas[z],[9] R. Culbertson,[15] N. d'Ascenzo[w],[15] M. Datta[qq],[15] P. De Barbaro,[45] L. Demortier,[46] M. Deninno,[6] M. d'Errico[ff],[40] F. Devoto,[21] A. Di Canto[gg],[42] B. Di Ruzza[q],[15] J.R. Dittmann,[5] M. D'Onofrio,[27] S. Donati[gg],[42] M. Dorigo[nn],[49] A. Driutti,[49] K. Ebina,[53] R. Edgar,[32] A. Elagin,[48] R. Erbacher,[7] S. Errede,[22] B. Esham,[22] R. Eusebi,[48] S. Farrington,[39] J.P. Fernández Ramos,[29] R. Field,[16] G. Flanagan[u],[15] R. Forrest,[7] M. Franklin,[20] J.C. Freeman,[15] H. Frisch,[11] Y. Funakoshi,[53] A.F. Garfinkel,[44] P. Garosi[hh],[42] H. Gerberich,[22] E. Gerchtein,[15] S. Giagu,[47] V. Giakoumopoulou,[3] K. Gibson,[43] C.M. Ginsburg,[15] N. Giokaris,[3] P. Giromini,[17] G. Giurgiu,[23] V. Glagolev,[13] D. Glenzinski,[15] M. Gold,[35] D. Goldin,[48] A. Golossanov,[15] G. Gomez,[9] G. Gomez-Ceballos,[30] M. Goncharov,[30] O. González López,[29] I. Gorelov,[35] A.T. Goshaw,[14] K. Goulianos,[46] E. Gramellini,[6] S. Grinstein,[4] C. Grosso-Pilcher,[11] R.C. Group[52],[15] J. Guimaraes da Costa,[20] S.R. Hahn,[15] J.Y. Han,[45] F. Happacher,[17] K. Hara,[50] M. Hare,[51] R.F. Harr,[54] T. Harrington-Taber[n],[15] K. Hatakeyama,[5] C. Hays,[39] J. Heinrich,[41] M. Herndon,[55] A. Hocker,[15] Z. Hong,[48] W. Hopkins[g],[15] S. Hou,[1] R.E. Hughes,[36] U. Husemann,[56] M. Hussein[dd],[33] J. Huston,[33] G. Introzzi[mm],[42] M. Iori[jj],[47] A. Ivanov[p],[7] E. James,[15] D. Jang,[10] B. Jayatilaka,[15] E.J. Jeon,[25] S. Jindariani,[15] M. Jones,[44] K.K. Joo,[25] S.Y. Jun,[10] T.R. Junk,[15] M. Kambeitz,[24] T. Kamon[25],[48] P.E. Karchin,[54] A. Kasmi,[5] Y. Kato[o],[38] W. Ketchum[rr],[11] J. Keung,[41] B. Kilminster[oo],[15] D.H. Kim,[25] H.S. Kim,[25] J.E. Kim,[25] M.J. Kim,[17] S.B. Kim,[25] S.H. Kim,[50] Y.J. Kim,[25] Y.K. Kim,[11] N. Kimura,[53] M. Kirby,[15] K. Knoepfel,[15] K. Kondo*,[53] D.J. Kong,[25] J. Konigsberg,[16] A.V. Kotwal,[14] M. Kreps,[24] J. Kroll,[41] M. Kruse,[14] T. Kuhr,[24] M. Kurata,[50] A.T. Laasanen,[44] S. Lammel,[15] M. Lancaster,[28] K. Lannon[y],[36] G. Latino[hh],[42] H.S. Lee,[25] J.S. Lee,[25] S. Leo,[42] S. Leone,[42] J.D. Lewis,[15] A. Limosani[t],[14] E. Lipeles,[41] A. Lister[a],[18] H. Liu,[52] Q. Liu,[44] T. Liu,[15] S. Lockwitz,[56] A. Loginov,[56] A. Lucà,[17] D. Lucchesi[ff],[40] J. Lueck,[24] P. Lujan,[26] P. Lukens,[15] G. Lungu,[46] J. Lys,[26] R. Lysak[e],[12] R. Madrak,[15] P. Maestro[hh],[42] S. Malik,[46] G. Manca[b],[27] A. Manousakis-Katsikakis,[3] F. Margaroli,[47] P. Marino[ii],[42] M. Martínez,[4] K. Matera,[22] M.E. Mattson,[54] A. Mazzacane,[15] P. Mazzanti,[6] R. McNulty[j],[27] A. Mehta,[27] P. Mehtala,[21] C. Mesropian,[46] T. Miao,[15] D. Mietlicki,[32] A. Mitra,[1] H. Miyake,[50] S. Moed,[15] N. Moggi,[6] C.S. Moon[aa],[15] R. Moore[pp],[15] M.J. Morello[ii],[42] A. Mukherjee,[15] Th. Muller,[24] P. Murat,[15] M. Mussini[ee],[6] J. Nachtman[n],[15] Y. Nagai,[50] J. Naganoma,[53] I. Nakano,[37] A. Napier,[51] J. Nett,[48] C. Neu,[52] T. Nigmanov,[43] L. Nodulman,[2] S.Y. Noh,[25] O. Norniella,[22] L. Oakes,[39] S.H. Oh,[14] Y.D. Oh,[25] I. Oksuzian,[52] T. Okusawa,[38] R. Orava,[21] L. Ortolan,[4] C. Pagliarone,[49] E. Palencia[f],[9] P. Palni,[35] V. Papadimitriou,[15] W. Parker,[55] G. Pauletta[kk],[49] M. Paulini,[10] C. Paus,[30] T.J. Phillips,[14] G. Piacentino,[42] E. Pianori,[41] J. Pilot,[36] K. Pitts,[22] C. Plager,[8] L. Pondrom,[55] S. Poprocki[g],[15] K. Potamianos,[26] A. Pranko,[26] F. Prokoshin[cc],[13] F. Ptohos[h],[17] G. Punzi[gg],[42] N. Ranjan,[44] I. Redondo Fernández,[29] P. Renton,[39] M. Rescigno,[47] F. Rimondi*,[6] L. Ristori[42],[15] A. Robson,[19] T. Rodriguez,[41] S. Rolli[i],[51] M. Ronzani[gg],[42] R. Roser,[15] J.L. Rosner,[11] F. Ruffini[hh],[42] A. Ruiz,[9] J. Russ,[10] V. Rusu,[15] W.K. Sakumoto,[45] Y. Sakurai,[53] L. Santi[kk],[49] K. Sato,[50] V. Saveliev[w],[15] A. Savoy-Navarro[aa],[15] P. Schlabach,[15] E.E. Schmidt,[15] T. Schwarz,[32] L. Scodellaro,[9] F. Scuri,[42] S. Seidel,[35] Y. Seiya,[38] A. Semenov,[13] F. Sforza[gg],[42] S.Z. Shalhout,[7] T. Shears,[27] P.F. Shepard,[43] M. Shimojima[v],[50] M. Shochet,[11] I. Shreyber-Tecker,[34] A. Simonenko,[13] P. Sinervo,[31] K. Sliwa,[51] J.R. Smith,[7] F.D. Snider,[15] H. Song,[43] V. Sorin,[4] M. Stancari,[15] R. St. Denis,[19] B. Stelzer,[31] O. Stelzer-Chilton,[31] D. Stentz[x],[15] J. Strologas,[35] Y. Sudo,[50] A. Sukhanov,[15] I. Suslov,[13] K. Takemasa,[50] Y. Takeuchi,[50] J. Tang,[11] M. Tecchio,[32] P.K. Teng,[1] J. Thom[g],[15] E. Thomson,[41] V. Thukral,[48] D. Toback,[48] S. Tokar,[12] K. Tollefson,[33] T. Tomura,[50] D. Tonelli[f],[15] S. Torre,[17] D. Torretta,[15] P. Totaro,[40] M. Trovato[ii],[42] F. Ukegawa,[50] S. Uozumi,[25] F. Vázquez[m],[16] G. Velev,[15] C. Vellidis,[15]

Operated by Fermi Research Alliance, LLC under Contract No. De-AC02-07CH11359 with the United States Department of Energy.

C. Vernieri[ii],[42] M. Vidal,[44] R. Vilar,[9] J. Vizán[ll],[9] M. Vogel,[35] G. Volpi,[17] P. Wagner,[41] R. Wallny,[8] S.M. Wang,[1] A. Warburton,[31] D. Waters,[28] W.C. Wester III,[15] D. Whiteson[c],[41] A.B. Wicklund,[2] S. Wilbur,[11] H.H. Williams,[41] J.S. Wilson,[32] P. Wilson,[15] B.L. Winer,[36] P. Wittich[g],[15] S. Wolbers,[15] H. Wolfe,[36] T. Wright,[32] X. Wu,[18] Z. Wu,[5] K. Yamamoto,[38] D. Yamato,[38] T. Yang,[15] U.K. Yang[r],[11] Y.C. Yang,[25] W.-M. Yao,[26] G.P. Yeh,[15] K. Yi[n],[15] J. Yoh,[15] K. Yorita,[53] T. Yoshida[l],[38] G.B. Yu,[14] I. Yu,[25] A.M. Zanetti,[49] Y. Zeng,[14] C. Zhou,[14] and S. Zucchelli[ee6]

(CDF Collaboration[†])

[1]*Institute of Physics, Academia Sinica, Taipei, Taiwan 11529, Republic of China*
[2]*Argonne National Laboratory, Argonne, Illinois 60439, USA*
[3]*University of Athens, 157 71 Athens, Greece*
[4]*Institut de Fisica d'Altes Energies, ICREA, Universitat Autonoma de Barcelona, E-08193, Bellaterra (Barcelona), Spain*
[5]*Baylor University, Waco, Texas 76798, USA*
[6]*Istituto Nazionale di Fisica Nucleare Bologna,* [ee]*University of Bologna, I-40127 Bologna, Italy*
[7]*University of California, Davis, Davis, California 95616, USA*
[8]*University of California, Los Angeles, Los Angeles, California 90024, USA*
[9]*Instituto de Fisica de Cantabria, CSIC-University of Cantabria, 39005 Santander, Spain*
[10]*Carnegie Mellon University, Pittsburgh, Pennsylvania 15213, USA*
[11]*Enrico Fermi Institute, University of Chicago, Chicago, Illinois 60637, USA*
[12]*Comenius University, 842 48 Bratislava, Slovakia; Institute of Experimental Physics, 040 01 Kosice, Slovakia*
[13]*Joint Institute for Nuclear Research, RU-141980 Dubna, Russia*
[14]*Duke University, Durham, North Carolina 27708, USA*
[15]*Fermi National Accelerator Laboratory, Batavia, Illinois 60510, USA*
[16]*University of Florida, Gainesville, Florida 32611, USA*
[17]*Laboratori Nazionali di Frascati, Istituto Nazionale di Fisica Nucleare, I-00044 Frascati, Italy*
[18]*University of Geneva, CH-1211 Geneva 4, Switzerland*
[19]*Glasgow University, Glasgow G12 8QQ, United Kingdom*
[20]*Harvard University, Cambridge, Massachusetts 02138, USA*
[21]*Division of High Energy Physics, Department of Physics, University of Helsinki and Helsinki Institute of Physics, FIN-00014, Helsinki, Finland*
[22]*University of Illinois, Urbana, Illinois 61801, USA*
[23]*The Johns Hopkins University, Baltimore, Maryland 21218, USA*
[24]*Institut für Experimentelle Kernphysik, Karlsruhe Institute of Technology, D-76131 Karlsruhe, Germany*
[25]*Center for High Energy Physics: Kyungpook National University, Daegu 702-701, Korea; Seoul National University, Seoul 151-742, Korea; Sungkyunkwan University, Suwon 440-746, Korea; Korea Institute of Science and Technology Information, Daejeon 305-806, Korea; Chonnam National University, Gwangju 500-757, Korea; Chonbuk National University, Jeonju 561-756, Korea; Ewha Womans University, Seoul, 120-750, Korea*
[26]*Ernest Orlando Lawrence Berkeley National Laboratory, Berkeley, California 94720, USA*
[27]*University of Liverpool, Liverpool L69 7ZE, United Kingdom*
[28]*University College London, London WC1E 6BT, United Kingdom*
[29]*Centro de Investigaciones Energeticas Medioambientales y Tecnologicas, E-28040 Madrid, Spain*
[30]*Massachusetts Institute of Technology, Cambridge, Massachusetts 02139, USA*
[31]*Institute of Particle Physics: McGill University, Montréal, Québec H3A 2T8, Canada; Simon Fraser University, Burnaby, British Columbia V5A 1S6, Canada; University of Toronto, Toronto, Ontario M5S 1A7, Canada; and TRIUMF, Vancouver, British Columbia V6T 2A3, Canada*
[32]*University of Michigan, Ann Arbor, Michigan 48109, USA*
[33]*Michigan State University, East Lansing, Michigan 48824, USA*
[34]*Institution for Theoretical and Experimental Physics, ITEP, Moscow 117259, Russia*
[35]*University of New Mexico, Albuquerque, New Mexico 87131, USA*
[36]*The Ohio State University, Columbus, Ohio 43210, USA*
[37]*Okayama University, Okayama 700-8530, Japan*
[38]*Osaka City University, Osaka 588, Japan*
[39]*University of Oxford, Oxford OX1 3RH, United Kingdom*
[40]*Istituto Nazionale di Fisica Nucleare, Sezione di Padova-Trento,* [ff]*University of Padova, I-35131 Padova, Italy*
[41]*University of Pennsylvania, Philadelphia, Pennsylvania 19104, USA*
[42]*Istituto Nazionale di Fisica Nucleare Pisa,* [gg]*University of Pisa,* [hh]*University of Siena and* [ii]*Scuola Normale Superiore, I-56127 Pisa, Italy,* [mm]*INFN Pavia and University of Pavia, I-27100 Pavia, Italy*
[43]*University of Pittsburgh, Pittsburgh, Pennsylvania 15260, USA*
[44]*Purdue University, West Lafayette, Indiana 47907, USA*

[45]University of Rochester, Rochester, New York 14627, USA
[46]The Rockefeller University, New York, New York 10065, USA
[47]Istituto Nazionale di Fisica Nucleare, Sezione di Roma 1,
[jj]Sapienza Università di Roma, I-00185 Roma, Italy
[48]Mitchell Institute for Fundamental Physics and Astronomy,
Texas A&M University, College Station, Texas 77843, USA
[49]Istituto Nazionale di Fisica Nucleare Trieste/Udine; [nn]University of Trieste,
I-34127 Trieste, Italy; [kk]University of Udine, I-33100 Udine, Italy
[50]University of Tsukuba, Tsukuba, Ibaraki 305, Japan
[51]Tufts University, Medford, Massachusetts 02155, USA
[52]University of Virginia, Charlottesville, Virginia 22906, USA
[53]Waseda University, Tokyo 169, Japan
[54]Wayne State University, Detroit, Michigan 48201, USA
[55]University of Wisconsin, Madison, Wisconsin 53706, USA
[56]Yale University, New Haven, Connecticut 06520, USA

(Dated: April 30, 2013)

We present a measurement of the top-quark pair production cross-section in proton-antiproton collisions at $\sqrt{s}$=1.96 TeV. The data were collected at the Fermilab Tevatron by the CDF II detector and correspond to an integrated luminosity of 8.8 fb^{-1}, representing the complete CDF Run II data set. We select events consistent with the production of top-quark pairs by requiring the presence of two reconstructed leptons, an imbalance in the total event transverse momentum, and jets. At least one jet is required to be identified as consistent with the fragmentation of a bottom quark using a secondary-vertex-finding algorithm. The 246 candidate events are estimated to have a signal purity of 91%. We measure a cross section of $\sigma_{t\bar{t}}$ = 7.09 ± 0.84 pb, assuming a top-quark mass of 172.5 GeV/c^2. The results are consistent with the standard model as predicted by next-to-leading-order calculations.

PACS numbers: 13.85.Ni, 13.85.Qk, 14.65.Ha

Beginning with the discovery of the top quark (t) in 1995 [1, 2], the CDF and D0 experiments at Fermilab have studied its production, decays, and intrinsic properties [3–8]. This Letter continues that rich program by reporting the first top-antitop quark pair ($t\bar{t}$) production cross-section measurement by a Tevatron experiment that utilizes the complete Run II data set. Studies of the top quark provide both measurements of standard model (SM) parameters [9] and probes of non-SM particles or interactions [10]. Top-quark pairs are produced in proton-antiproton collisions at $\sqrt{s}$ = 1.96 TeV by the Fermilab Tevatron. We select events for this measurement if both leptons in the decay chain $t\bar{t} \to (W^+b)(W^-\bar{b}) \to (\ell^+\nu_l b)(\ell^-\bar{\nu}_l\bar{b})$ are identified. Only reconstructed electron or muon candidates are selected as leptons. Hadronic decays of tau leptons are not considered. The signal yield is measured as the number of selected events in the data after subtraction of the background expectation from other SM sources, and the cross section is measured by correcting the signal yield for acceptance, efficiency, and luminosity. This analysis uses the full CDF Run II data set collected between March 2002 and September 2011, which corresponds to 8.8 fb^{-1} of integrated luminosity after data-quality requirements are imposed. The result supersedes a previous analysis [5] by exploiting a three-fold increase in data set and improved $t\bar{t}$ signal-to-background ratio. Improved sample purity is obtained by requiring the presence of jets consistent with the fragmentation of b quarks (b-tagged jets) from the top quark

*Deceased
†With visitors from [a]University of British Columbia, Vancouver, BC V6T 1Z1, Canada, [b]Istituto Nazionale di Fisica Nucleare, Sezione di Cagliari, 09042 Monserrato (Cagliari), Italy, [c]University of California Irvine, Irvine, CA 92697, USA, [e]Institute of Physics, Academy of Sciences of the Czech Republic, 182 21, Czech Republic, [f]CERN, CH-1211 Geneva, Switzerland, [g]Cornell University, Ithaca, NY 14853, USA, [dd]The University of Jordan, Amman 11942, Jordan, [h]University of Cyprus, Nicosia CY-1678, Cyprus, [i]Office of Science, U.S. Department of Energy, Washington, DC 20585, USA, [j]University College Dublin, Dublin 4, Ireland, [k]ETH, 8092 Zürich, Switzerland, [l]University of Fukui, Fukui City, Fukui Prefecture, Japan 910-0017, [m]Universidad Iberoamericana, Lomas de Santa Fe, México, C.P. 01219, Distrito Federal, [n]University of Iowa, Iowa City, IA 52242, USA, [o]Kinki University, Higashi-Osaka City, Japan 577-8502, [p]Kansas State University, Manhattan, KS 66506, USA, [q]Brookhaven National Laboratory, Upton, NY 11973, USA, [r]University of Manchester, Manchester M13 9PL, United Kingdom, [s]Queen Mary, University of London, London, E1 4NS, United Kingdom, [t]University of Melbourne, Victoria 3010, Australia, [u]Muons, Inc., Batavia, IL 60510, USA, [v]Nagasaki Institute of Applied Science, Nagasaki 851-0193, Japan, [w]National Research Nuclear University, Moscow 115409, Russia, [x]Northwestern University, Evanston, IL 60208, USA, [y]University of Notre Dame, Notre Dame, IN 46556, USA, [z]Universidad de Oviedo, E-33007 Oviedo, Spain, [aa]CNRS-IN2P3, Paris, F-75205 France, [cc]Universidad Tecnica Federico Santa Maria, 110v Valparaiso, Chile, [ll]Universite catholique de Louvain, 1348 Louvain-La-Neuve, Belgium, [oo]University of Zürich, 8006 Zürich, Switzerland, [pp]Massachusetts General Hospital and Harvard Medical School, Boston, MA 02114 USA, [qq]Hampton University, Hampton, VA 23668, USA, [rr]Los Alamos National Laboratory, Los Alamos, NM 87544, USA

decay.

The CDF II detector is a solenoidal spectrometer surrounded by a sampling calorimeter and muon detectors [11]. CDF uses a cylindrical coordinate system in which θ is the polar angle about an axis defined by the proton beam and ϕ is the azimuthal angle about the beam axis. The events were selected for analysis during data taking (triggered) with an inclusive selection that required the presence of an electron (a muon) with $E_T > 18$ GeV ($p_T >$ 18 GeV/c). The transverse energy and momentum are defined as $E_T = E\sin(\theta)$ and $p_T = p\sin(\theta)$ where E is the energy measured in the calorimeter and p is the momentum measured by the tracking system. In the offline analysis, we select events that contain at least one isolated [12] electron (muon) with E_T $>$ 20 GeV ($p_T >$ 20 GeV/c). We additionally require the presence of a second lepton with the same energy requirements, but without isolation requirements. Events with more than two reconstructed leptons are rejected.

The neutrinos from dilepton top-quark pair decays escape detection, so signal events are expected to produce a large imbalance in the event total transverse-energy ($\not\!\!E_{\rm T}$) [13] compared to other SM processes containing two leptons. We require $\not\!\!E_{\rm T} > 25$ GeV to reduce contamination from processes that do not involve neutrinos from vector-boson decays. Events in which $\not\!\!E_{\rm T}$ originates from instrumental effects typically feature a small angle between the direction of a lepton or jet and the direction of $\vec{\not\!\!E}_{\rm T}$. If this angle is smaller than 20°, we require $\not\!\!E_{\rm T} >$ 50 GeV to reject these backgrounds. To specifically reject events from Z/γ^* production, we require high $\not\!\!E_{\rm T}$ significance [5] if the identified leptons have the same flavor and dilepton mass consistent with the Z resonance. We also require the dilepton mass to be larger than 5 GeV/c^2 to remove events from low-mass dimuon resonances. The resulting sample is referred to as events meeting the *dilepton selection*. Jets are identified in the CDF frame using a modified cone algorithm [14], and are defined as having $E_T >$15 GeV and pseudorapidity in the lab frame satisfying $|\eta| < 2.5$. Events satisfying the dilepton selection that contain exactly zero or one jet are used as control samples for background estimation. The *pretag sample* contains events passing the dilepton selection with at least two jets, summed transverse energy over all particles (H_T) satisfying $H_T > 200$ GeV, and whose two leptons are of opposite electric charge. The data sample corresponds to an integrated luminosity of 9.1 fb^{-1}, slightly higher than the signal sample, because the detector quality requirements for b tagging are not imposed. The pretag sample is used to validate the signal and background models. We measure the $t\bar{t}$ production cross-section using the *tag sample*, which is the subset of pretag events in which at least one of the jets in the event is b tagged by the SECVTX algorithm [15].

The lifetime of B hadrons is approximately 1.5 picosecond, so relativistic B hadrons produced in collisions at the Tevatron can travel on the order of 450 micrometers from the primary interaction-point (primary vertex) before decaying. We use charged-particle tracks to reconstruct the primary vertex and secondary decay-vertices. We then compute the two-dimensional displacement of the secondary vertex from the primary vertex projected along the jet direction in the plane transverse to the beam (L_{2D}). A jet is considered b-tagged by the SECVTX algorithm if L_{2D} and its uncertainty (σ) satisfy the significance $L_{2D}/\sigma > 7.5$. Jets with $L_{2D}/\sigma < -7.5$ are not topologically consistent with B-hadron decays, but are used to estimate the false-tag rate due to instrumental sources [15].

Selection efficiency for $t\bar{t}$ events is estimated using the PYTHIA Monte Carlo event-generator [16] combined with a detailed simulation of the CDF II detector [17]. The $t\bar{t}$ signal is simulated assuming a top-quark mass of 172.5 GeV/c^2 and only contains events in which both W bosons produced by the decay of the top quarks subsequently decay into a charged lepton (e, μ, τ) and a neutrino. Only simulated events with a primary vertex reconstructed within $\pm$60 cm of the nominal CDF detector center are retained. This requirement has an efficiency of [97.47 $\pm$ 0.02(stat)]% of the full CDF luminous region. The total acceptance for the b-tagged (pretag) dilepton signal events is [0.461 $\pm$ 0.003(stat)]% ([0.756 $\pm$ 0.004(stat)]%), including the branching fraction to leptons. The efficiency for simulated $t\bar{t}$ events is then corrected for high-transverse-energy electron and muon identification, using multiplicative factors that are measured by selecting Z-boson decays to leptons, in which one of the leptons from the decay is minimally biased by the Z-boson event selection. The simulation is also corrected for observed differences between experimental and simulated data due to the efficiency of the inclusive lepton trigger, which is measured using data samples selected by an independent set of triggering criteria. We correct for the difference in efficiency for the b-tagging algorithm between data and simulated samples by using a multiplicative correction factor, $S_b = 0.96 \pm 0.05$. This correction accounts for the differences between properties of jets in $t\bar{t}$ events and jets in the b-tagging calibration sample [15].

The relevant background processes yielding prompt lepton pairs are diboson (WW, WZ, and ZZ) production and Z/γ^* production. Processes in which a photon or hadronic fragmentation are identified as a lepton are also considered, such as $W\gamma$ and W boson production in association with multiple jets. The signal sample contamination is predicted to predominantly comprise Z/γ^* and W+jets production processes, so their normalizations are estimated using data samples enriched in these processes. The contamination for the remaining backgrounds is predicted using the same detector simulation and corrections used for signal.

Diboson production is simulated with PYTHIA, normalized to the production cross-sections from the next-to-leading order calculations using MCFM [18] and MSTW2008 [19] parton distribution functions (PDF). The predicted cross sections are $\sigma_{WW} = 11.34 \pm 0.68$ pb, $\sigma_{WZ} = 3.47 \pm 0.21$ pb, and $\sigma_{ZZ} = 3.62 \pm 0.22$ pb [20]. The σ_{WZ} and σ_{ZZ} values are computed by restricting the phase space to dilepton masses greater than 2 GeV/c^2. The $Z/\gamma^* \to \ell^+\ell^-$ production is simulated using the ALPGEN+PYTHIA event generator [21]. The $Z/\gamma^* \to e^+e^-$, $\mu^+\mu^-$ samples, which are only selected due to instrumental mismeasurements, are normalized in a data derived process. The process $Z \to \tau^+\tau^-$ has significant $\not\!\!E_{\rm T}$ from neutrinos, and is treated separately; it is normalized to the ALPGEN production rate, corrected for next-to-leading-order contributions [5]. The $W\gamma$ decays are simulated with the BAUR event generator [22], assuming a leading-order production cross-section of $\sigma_{W\gamma} = 32 \pm 3$ pb and correcting for higher-order effects [23]. This process is observed to be relevant in low jet-multiplicity control samples, and negligible in the signal sample.

The WW and $Z/\gamma^* \to \tau\tau$ jet multiplicity spectra are corrected to account for discrepancies observed between data and simulation in Z boson decays, using jet-multiplicity-dependent correction factors. The corrections are applied to processes in which jets are produced by initial-state radiation, rather than from final-state partons in the hard scattering. The uncertainties on the acceptances of the simulated background processes come from the convolution of the uncertainties due to finite simulation sample-size and uncertainties on the jet-multiplicity correction factors, lepton identification, and jet energy scale [24].

The sample contamination from Z/γ^* to ee and $\mu\mu$ decays with instrumental missing energy is estimated in a data sample in which the dilepton mass for all events is consistent with the Z resonance, but all other selection criteria are that of the pretag sample. We subtract the contributions from other processes, and then extrapolate the observed rate outside of the resonance region by using simulated samples, independently for each lepton type and jet-multiplicity. The uncertainty on this background contribution is dominated by the limited number of Z/γ^* data events with high $\not\!\!E_{\rm T}$ used to normalize the overall prediction, from the finite size of the Z/γ^* events that meet the selection, and from the uncertainty on the jet-energy scale. The normalization of the $Z/\gamma^* + u, d, s, g$ event yield in the tagged sample is determined by applying the scalings determined in the pretag sample, and applying false b-tag rates [15] as weights to the ALPGEN+PYTHIA events. We obtain the $Z/\gamma^* + b, c$ event yield normalization in the tagged sample by requiring events with dilepton mass consistent with the Z resonance, but all other selection criteria as that of the tag sample. After subtracting the estimated $Z/\gamma^* + u, d, s, g$ component and other backgrounds, the multiplicative heavy-flavor-specific Z/γ^* normalization corrections are found to be 1.8 ± 0.1.

We estimate a small contribution to the sample of events with one electron and one muon from $Z/\gamma^* \to \mu\mu$ events, in which bremsstrahlung associated with one muon mimics an electron signature. These events are described using the $Z/\gamma^* \to \mu\mu$ simulation sample.

The background from jets misidentified as leptons is estimated by using data events with exactly one identified lepton and additional lepton candidates that satisfy less restrictive identification criteria. The probability that a lepton-like candidate is reconstructed as a lepton is parametrized in terms of the candidate's transverse energy and isolation, and measured in large samples of events triggered by the presence of at least one jet. Misidentified leptons are modeled by applying these probabilities as weights to data events with only one high transverse-energy reconstructed lepton and a second electron-like or muon-like candidate. To remove events with two leptons from this sample, the lepton-like candidate is required to fail at least one lepton identification requirement. The misidentified-lepton events are required to meet all event selection requirements when treating the lepton-like candidates as the second lepton in the event. The uncertainty on the misidentified-lepton background model is dominated by the differences observed between identification rates determined in jet samples triggered by jets with E_T greater than 20, 50, 70, or 100 GeV.

A common systematic uncertainty for signal and simulated background estimates comes from the uncertainty on the lepton identification correction factors, which is measured to be 2.2%. The 3.3% uncertainty due to the jet-energy scale affects all simulated samples, and is estimated by varying the jet-energy corrections by $\pm 1\sigma$ of their systematic uncertainty and measuring the shift in signal and background acceptance. We consider several other sources of systematic uncertainties predominantly affecting the signal efficiency: difference in $t\bar{t}$ modeling by various simulation generators, simulation of initial- and final-state radiation, color reconnection, and PDF [19] uncertainty. These are determined by comparing the uncorrected simulation acceptance of the default $t\bar{t}$ PYTHIA sample to specialized simulation samples. The uncertainty due to each of these sources is estimated to be less than 2.0%. The systematic uncertainty due to the b-tagging efficiency correction is 5.0%, dominated by the light-flavor modeling. All simulated backgrounds have uncertainty due to the jet-multiplicity correction factor. Uncorrelated sources of systematic uncertainties affecting individual backgrounds include the 30% systematic uncertainty on the misidentified lepton contamination and individual theoretical uncertainties, ranging from 2% to 10%, on the production cross-sections of diboson and $Z \to \tau\tau$ processes. Each of these effects contributes to only a small fraction of the resulting 2.1% (7.1%) background systematic uncertainty for the b-tagged (pretag) sample. Table I summarizes the systematic uncertainties that affect the signal acceptance and background model [5].

TABLE I: Systematic uncertainties for the pretag and b-tagged samples. The total systematic uncertainty is the sum in quadrature of each independent contribution.

Source	Uncertainty (%)	
	Pretag	b-tagged
Lepton identification efficiency	2.2	2.2
Jet energy scale	3.3	3.3
Simulated event generator	1.9	1.9
Initial- and final-state radiation	1.3	1.3
Color reconnection	1.2	1.2
PDF	0.6	0.6
b-tagging	-	5.0
Background model	7.1	2.1
Total systematic uncertainty	8.6	7.2

The expected and observed background events that are b-tagged in the 1-jet sample are used as a control sample. The final sample of events with two or more jets passing all candidate selection criteria is given in Table II. The signal purity in the tag sample is 91%, which can be compared to the 73% achieved in the pretag sample. In Fig. 1, we present the jet E_T spectrum for the leading two jets in events with at least two jets, and at least one b-tag. The signal yield in the figure is normalized to the measured cross section, and the shape of the distribution is well described by the prediction.

TABLE II: Estimated number of background and $t\bar{t}$ signal events in the b-tagged sample, which corresponds to an integrated luminosity of 8.8 fb^{-1}. The observed event yields are compared with the total SM expectation for both the 1-jet and signal samples. The quoted uncertainties are the quadratic sum of the statistical and systematic uncertainties in each row. In the right column, "H_T+OS"refers to the requirements that events posses leptons with opposite electric charge sign and satisfy $H_T > 200$ GeV. These requirements are not applied to the events in the left column.

Source	1 jet (Validation region)	≥ 2 jets (H_T+OS) (Signal region)
hline WW	0.8 ± 0.2	0.6 ± 0.2
WZ	0.2 ± 0.0	0.1 ± 0.0
ZZ	0.1 ± 0.0	0.3 ± 0.1
$Z/\gamma^* + u, d, s, g$	2.1 ± 0.2	2.8 ± 0.3
$Z/\gamma^* + b, c$	1.8 ± 0.2	2.5 ± 0.2
Other	1.9 ± 0.7	15.6 ± 4.6
Total background	6.9 ± 0.9	21.9 ± 4.7
$t\bar{t}$ ($\sigma = 7.09$ pb)	20.2 ± 1.4	224.1 ± 15.5
Total SM expectation	27.1 ± 2.2	246.0 ± 19.9
Observed	29	246

The measured cross section is calculated as

$$\sigma_{t\bar{t}} = \frac{\mathrm{N_{obs}} - \mathrm{N_{bkg}}}{\sum_i \mathcal{A}_i \mathcal{L}_i}, \quad (1)$$

where $\mathrm{N_{obs}}$ is the number of dilepton candidate events, $\mathrm{N_{bkg}}$ is the total number of expected background events, and the denominator is the weighted sum of the corrected acceptance for each class of events grouped by lepton reconstruction. We multiply $\mathcal{A}_i$ by the integrated luminosity corresponding to the reconstruction class $\mathcal{L}_i$. Various values of integrated luminosities are used because the identification of events as belonging to each lepton class requires different CDF subdetectors to be fully functional. The total denominator for the b-tagged events is 31.60 ± 0.19 pb^{-1}.

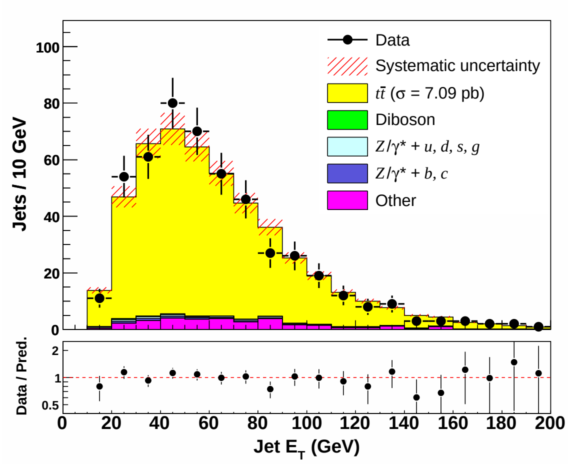

FIG. 1: Distribution of jet E_T values for the two jets with largest E_T in each event (black points) for the signal sample. The histogram represents the sum of the signal and background estimates, where the signal is normalized to the observed cross section. The hatched area is the total uncertainty on the sum of the signal and background predictions. The lower panehows the observed data yield divided by the predicted yield.

For the b-tagged $t\bar{t}$ dilepton sample, we measure a cross section of $\sigma_{t\bar{t}} = 7.09 \pm 0.49(\mathrm{stat}) \pm 0.52(\mathrm{syst}) \pm 0.43(\mathrm{lumi})$ pb $= 7.09 \pm 0.84$ pb with the 246 signal candidate events. The systematic uncertainty is the convolution of the acceptance and the background uncertainties shown in Table I. The 6% luminosity uncertainty is kept separate [25]. The results presented here are consistent with the best recent predictions from next-to-leading order theoretical calculations [10], and with previous D0 and CDF publications [4, 5]. The current data sample corresponds to an integrated luminosity three times greater than that of the previous publication [5], producing a result with statistical uncertainty reduced to less than that due to systematic effects. The use of b-jet identification further improves the signal purity from 73% to

91%, and the total uncertainty of the measurement has been improved from 1.04 pb in the previous CDF publication to the current value of 0.84 pb.

In conclusion, we have measured the production cross-section of top-quark pairs at the Tevatron, using the full CDF Run II data set. This measurement offers a robust addition to global combined measurements of the top-quark production cross-section, which can then be used as constraints to theoretical calculations and limits on non-SM contributions in the top-quark sector.

We thank the Fermilab staff and the technical staffs of the participating institutions for their vital contributions. This work was supported by the U.S. Department of Energy and National Science Foundation; the Italian Istituto Nazionale di Fisica Nucleare; the Ministry of Education, Culture, Sports, Science and Technology of Japan; the Natural Sciences and Engineering Research Council of Canada; the National Science Council of the Republic of China; the Swiss National Science Foundation; the A.P. Sloan Foundation; the Bundesministerium für Bildung und Forschung, Germany; the Korean World Class University Program, the National Research Foundation of Korea; the Science and Technology Facilities Council and the Royal Society, UK; the Russian Foundation for Basic Research; the Ministerio de Ciencia e Innovación, and Programa Consolider-Ingenio 2010, Spain; the Slovak R&D Agency; the Academy of Finland; the Australian Research Council (ARC); and the EU community Marie Curie Fellowship contract 302103.

[1] F. Abe *et al.* (CDF Collaboration), Phys. Rev. Lett. **74**, 2626 (1995).
[2] S. Abachi *et al.* (D0 Collaboration), Phys. Rev. Lett. **74**, 2632 (1995).
[3] T. Aaltonen *et al.* (CDF and D0 Collaborations), Phys. Rev. D **86**, 092003 (2012); T. Aaltonen *et al.* (CDF Collaboration), Phys. Rev. Lett. **109**, 152003 (2012).
[4] V. M. Abazov *et al.* (D0 Collaboration), Phys. Lett. B **704**, 403 (2011).
[5] T. Aaltonen *et al.* (CDF Collaboration), Phys. Rev. D **82**, 052002 (2010).
[6] T. Aaltonen *et al.* (CDF Collaboration), Phys. Rev. D **84**, 031101 (2011).
[7] T. Aaltonen *et al.* (CDF and D0 Collaborations), Phys. Rev. D **85**, 071106 (2012); T. Aaltonen *et al.* (CDF Collaboration), Phys. Rev. D **87**, 031104(R) (2013).
[8] T. Aaltonen *et al.* (CDF Collaboration), Phys. Rev. Lett. **105**, 012001 (2010).
[9] ALEPH, CDF, D0, DELPHI, L3, OPAL, SLD Collaborations, LEP Electroweak Working Group, Tevatron Electroweak Working Group, SLD Electroweak and Heavy Flavour Groups, arXiv:1012.2367 and references therein.
[10] M. Cacciari, S. Frixione, M. L. Mangano, P. Nason, and G. Ridolfi, J. High Energy Phys. 09 (2008) 127; N. Kidonakis and R. Vogt, Phys. Rev. D **78**, 074005 (2008); S. Moch and P. Uwer, Nucl. Phys. Proc. Suppl. **183**, 75 (2008); M. Czakon, P. Fiedler, and A. Mitov, arXiv:1303.6254 [hep-ph].
[11] R. Blair *et al.* Fermilab-Pub-96/390-E; D. Acosta *et al.* (CDF Collaboration), Phys. Rev. D **71**, 032001 (2005).
[12] A. Abulencia *et al.* (CDF Collaboration), J. Phys. G **34**, 2457 (2007).
[13] The missing transverse energy $\not\!\!E_{\rm T}$ is defined to be $-\Sigma_i E_T^i \hat{\rm n}_i$ where i is the calorimeter tower number with $\mid \eta \mid < 3.6$, $\hat{\rm n}_i$ is a unit vector perpendicular to the beam axis and pointing at the ith calorimeter tower.
[14] A. Bhatti *et al.*, Nucl. Instrum. Methods Phys. Res. Sect. A **566** (2006) 375.
[15] D. Acosta *et al.* (CDF Collaboration), Phys. Rev. D **71**, 052003 (2005).
[16] T. Sjöstrand, S. Mrenna, and P. Skands, J. High Energy Phys. 05 (2006) 026. We use version 6.216.
[17] GEANT3, R. Brun, F. Bruyant, M. Maire, A. C. McPherson, and P. Zanarini, CERN Report No. CERN-DD/EE/84-1, (1987).
[18] J. M. Campbell and R. K. Ellis, Phys. Rev. D **60**, 113006 (1999).
[19] A. D. Martin, W. J. Stirling, R. S. Thorne, and G. Watt Eur. Phys. J. C **63**, 189 (2009).
[20] The diboson cross sections when $75 < m_{\ell^+\ell^-} < 105$ GeV/c^2 are $\sigma_{WZ} = 3.22 \pm 0.22$ pb and $\sigma_{ZZ} = 1.20 \pm 0.06$ pb. The values are calculated using MCFM, J. M. Campbell and R. K. Ellis, Phys. Rev. D **60**, 113006 (1999).
[21] M. L. Mangano, M. Moretti, F. Piccinini, R. Pittau, and A. D. Polosa, J. High Energy Phys. 07 (2003) 001. We use version 2.10.
[22] U. Baur and E. L. Berger, Phys. Rev. D **41**, 1476 (1990).
[23] U. Baur, T. Han, and J. Ohnemus, Phys. Rev. D **48**, 5140 (1993).
[24] A. Abulencia *et al.* (CDF Collaboration), Phys. Rev. D **73**, 032003 (2006); T. Aaltonen *et al.* (CDF Collaboration), Phys. Rev. D **81**, 052011 (2010).
[25] D. Acosta *et al.*, Nucl. Instrum. Methods Phys. Res. Sect. A **494**, 57 (2002).